Supporting Information for

Nonheme Oxoiron(IV) Complexes of Pentadentate N5 Ligands: Spectroscopy, Electrochemistry, and Oxidative Reactivity

Dong Wang,[‡] Kallol Ray,[‡,§] Michael J. Collins,[‡,±] Erik R. Farquhar,[‡] Jonathan R. Frisch,[‡] Laura Gómez,[^] Timothy A. Jackson,[‡] Marion Kerscher,[#] Arkadius Waleska,[#] Peter Comba,[#,] Miquel Costas,[^,*] and Lawrence Que, Jr.[‡,*]*

[‡] Department of Chemistry and Center for Metals in Biocatalysis, University of Minnesota, 207 Pleasant St. SE, Minneapolis MN 55455, USA.

[±] Department of Chemistry, Viterbo University, La Crosse, WI 54601, USA

[^] Departament de Química, Universitat de Girona, Campus de Montilivi, E-17071 Girona, Spain.

[#] Universität Heidelberg, Anorganisch-Chemisches Institut, INF 270, D-69120 Heidelberg, Germany.

[§] Current Address: Humboldt-Universität zu Berlin, Department of Chemistry, Brook-Taylor Str. 2, 12489 Berlin, Germany.

**e-mail: larryque@chem.umn.edu, peter.comba@aci.uni-heidelberg.de, miquel.costas@udg.edu*

Experimental Section

All chemicals obtained from Aldrich Chemical Co. were the best available purity and were used without further purification unless otherwise indicated. Solvents were dried according to published procedures and distilled under Ar prior to use.[1] Iodosylbenzene (PhIO) was prepared by a literature method.[2] Iron(II) complexes **1a,**[3] **2a**[4], **3a**,[5] **4a**[6] and **5a**[6] were prepared according to previously published methods. Corresponding oxoiron(IV) complexes **1** – **5** were prepared by reacting the respective iron(II) complexes with 5 equiv of solid PhIO in CH_3CN at ambient temperature and filtering off the unreacted PhIO.

UV-vis spectra were recorded on an HP 8453A diode array spectrometer equipped with a USP-203 cryostat from Unisoku Scientific Instruments, Osaka, Japan. Electrospray ionization mass spectral (ESI-MS) experiments were carried out on a Bruker BioTOF II mass spectrometer using the following conditions: spray chamber voltage = 4000 V; gas carrier temperature = 200 °C.

Resonance Raman spectra were collected using a Spectra-Physics Model 2060 krypton ion laser and an ACTON AM-506 monochromator equipped with a Princeton LN/CCD data collection system. Low temperature spectra in CH_3CN or CD_3CN were obtained at 77 K using a 135° backscattering geometry. Samples were frozen onto a gold-plated copper cold finger in thermal contact with a Dewar flask containing liquid nitrogen. Raman frequencies were calibrated to indene prior to data collection. The monochromator slit width was set for a band-pass of 4 cm^{-1} for all spectra. Our initial attempts to obtain resonance Raman spectra of **1** – **5** failed, because of their high susceptibility to photodecomposition upon laser excitation. The resonance Raman data presented in Table 1 were obtained by irradiation of fresh spots on the surfaces of the frozen samples in the course of spectral accumulation in order to obtain spectra of acceptable quality.

X-ray absorption spectroscopic data for **1**, **3**, **4**, and **5** were collected on beamlines X9B (**1**, **4**, and **5**) and X3B (**3**) of the National Synchrotron Light Source (NSLS) at Brookhaven National Laboratory, with storage ring conditions of 2.8 GeV and 100 – 300 mA. At NSLS, Fe K-edge XAS data were collected for frozen solution samples maintained at *ca.* 15 K over an energy range of 6.9 – 8.0 keV using a Si(111) double crystal monochromator for energy selection and a Displex closed cycle cryostat for temperature control. A bent focusing mirror was used for harmonic rejection. Data were obtained as fluorescence excitation spectra with a 13-

element solid-state germanium detector array (Canberra). An iron foil spectrum was recorded concomitantly for internal energy calibration and the first inflection point of the K-edge was assigned to 7112.0 eV. The Fe concentration, purity, and number of scans acquired for each XAS sample were as follows: **1**, 25 mM Fe, 90% Fe(IV) by UV/Vis, 6 scans; **3**, 18 mM Fe, 85% Fe(IV) by UV/Vis, 4 scans; **4**, 6.8 mM Fe, 74% Fe(IV) by UV/Vis, 13 scans; **5**, 13 mM Fe, 85% Fe(IV) by UV/Vis, 9 scans.

XAS data reduction, averaging, and normalization were performed using the program EXAFSPAK.[7] Following calibration and averaging of the data, background absorption was removed by fitting a Gaussian function to the pre-edge region and then subtracting this function from the entire spectrum. A three-segment spline with fourth order components was then fit to the EXAFS region of the spectrum in order to extract χ(k). Analysis of the pre-edge features was carried out with the program SSExafs[8] using a previously described protocol.[9] Theoretical phase and amplitude parameters for a given absorber-scatterer pair were calculated using FEFF 8.40[10] at the single-scattering level of theory, and were utilized by the opt program of the EXAFSPAK package during curve-fitting. In all analyses, the coordination number (*n*) of a given shell was a fixed parameter, and was varied iteratively while bond lengths (*r*) and Debye-Waller factors (σ^2) were allowed to freely float. The amplitude reduction factor S_0 was fixed at 0.9, while the edge shift parameter E_0 was allowed to float as a single value for all shells (thus in any given fit, the number of floating parameters = (2 × num shells) + 1). The goodness-of-fit parameter F was defined as $F = \Sigma(\chi_{exptl}-\chi_{calc})^2$, while *F*' is defined as $F^2 / (N_{IDP} - N_{VAR})$, where N_{IDP} is the number of independent data points and N_{VAR} is the number of floated variables in a given fit. *F*' is a test of whether addition of a shell is merited in the fit.[11]

All electrochemical experiments were performed using a Cypress system CS1200 analyzer. The cyclic voltammetric measurements were carried out in CH_3CN, containing iron complexes (1 mM) and tetrabutylammonium hexafluorophosphate ($TBAPF_6$, 0.1 M) as supporting electrolyte, using a glassy carbon working electrode, a $Ag/AgNO_3$ (0.05 M) reference electrode, and a platinum auxiliary electrode. All potentials are reported versus the Fc^+/Fc (Fc = ferrocene) couple. Spectropotentiometry experiments were carried out in a 1-cm rectangular cuvet containing a piece of 100 ppi reticulated vitreous carbon (RVC) as the working electrode cut to dimensions of 10 mm x 9 mm x 20 mm so as to fit into the cuvet. A 2 mm hole was drilled through the 10 mm side so as to be at the center of the spectrometer light path. Electrical contact

was made by means of a 20-gauge Pt wire pushed down one edge of the cuvet. The auxiliary electrode consisted of a Pt wire dipped in a glass tubing capped with a porous vycor tip and heat shrink tubing and filled with 0.1 M $TBAPF_6$ solution in CH_3CN. A no-leak Ag/AgCl reference electrode was used and 0.1 M $TBAPF_6$ was the supporting electrolyte.

In the spectropotentiometric titrations, the Fe(III) complexes were initially generated by applying a potential of 0.6 – 0.8 V to respective Fe(II) solutions (0.25 mM) in CH_3CN containing 0.1 M H_2O. The formation of the Fe(III) complexes was monitored by the appearance of the 300-450 nm bands in their UV-Vis spectra. The spectral changes were typically complete within 5 min for **2b**, **4b** and **5b**, and 15-20 min for **1b** and **3b**. The applied potential on the electrochemically generated iron(III) solutions in the cuvette was then incremented in 20-50 mV steps. Spectra were recorded at each potential every 60 seconds until there were essentially no changes in absorbance in the near-IR region corresponding to the oxoiron(IV) complexes. Typically a time period of 30-40 min was required to achieve equilibrium for each increment in potential. Nernst-equation fitting to the plots of absorbance vs. applied potential was performed according to previously published procedures.[12]

Kinetic studies were performed by adding appropriate amounts of substrates to 1 mM solutions of **1** – **5** in CH_3CN under completely anaerobic conditions, and spectral changes of the intermediates were directly monitored by a UV–vis spectrophotometer. Rate constants, k_{obs}, were determined by pseudo–first–order fitting of the decrease of the absorption bands at 696 nm for **1**, 739 nm for **2**, 740 nm for **3** and 730 nm for **4** and **5**. All the rate constants are averages of at least three determinations. Plots of the k_{obs} values versus substrate concentration afforded second order rate constants k_2. The kinetic traces for all reactions were fitted well with a first-order exponential decay model. Although some deviation from pseudo-first order behavior could be observed in the latter phases of some reactions, reasonable R^2 values were obtained for fits over three half-lives in all cases. Product analyses were performed on a Perkin-Elmer Sigma 3 gas chromatograph (AT-1701 column, 30 m) with a flame ionization detector. GC mass spectral analyses were performed on a HP 5898 GC (DB-5 column, 60 m) with a Finnigan MAT 95 mass detector or a HP 6890 GC (HP-5 column, 30 m) with an Agilent 5973 mass detector. A 4% NH_3/CH_4 mix was used as the ionization gas for chemical ionization analyses.

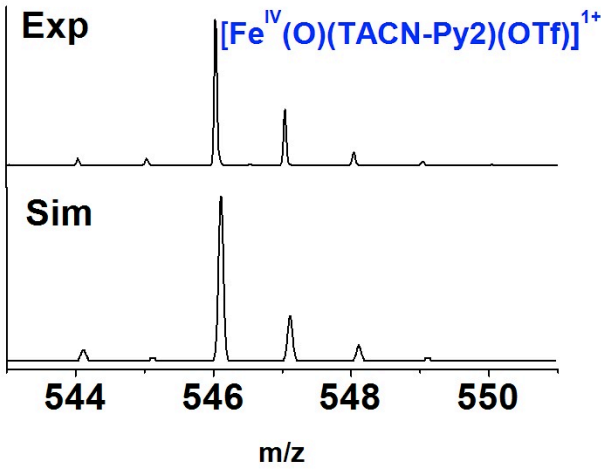

Figure S1. ESI-MS of **3** in CH_3CN.

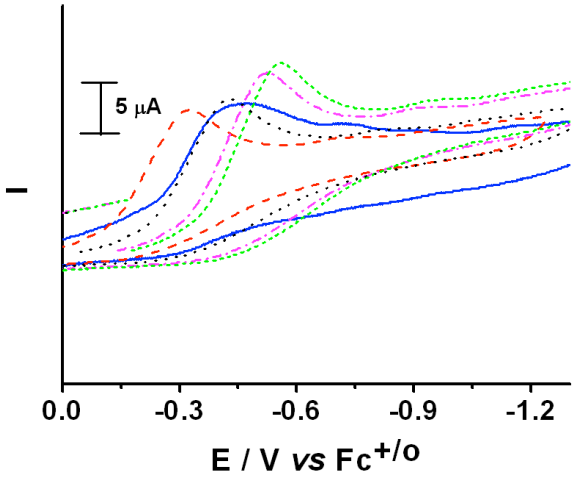

Figure S2. Cyclic voltammograms of 1 mM solutions of oxoiron(IV) complexes **1** (purple dash-dotted line), **2** (black dotted line), **3** (green short dashed line), **4** (blue solid line), and **5** (red long dashed line) in CH_3CN containing 0.1 M $TBAPF_6$ at 25 ^oC using a glassy carbon working electrode and Ag/AgCl reference electrode. Scan rate 0.25 V s^{-1}.

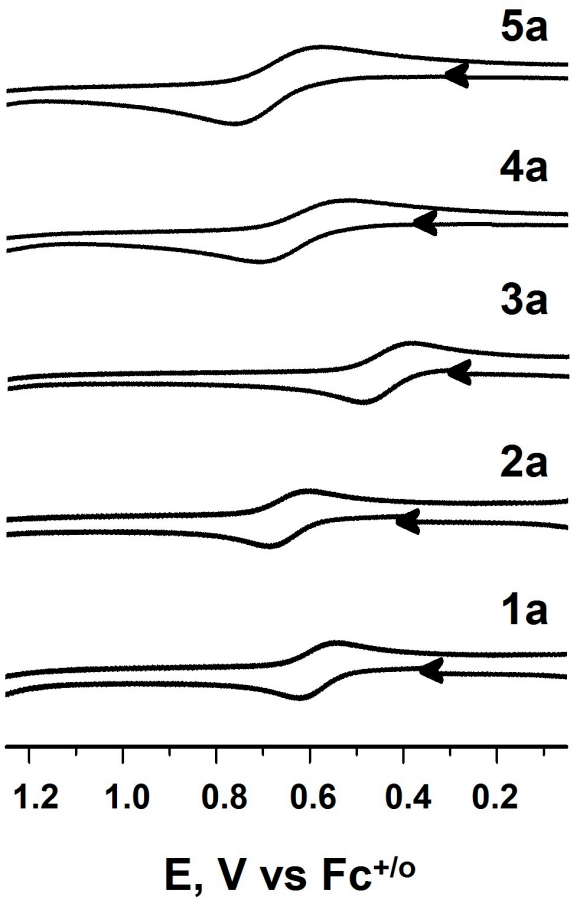

Figure S3. Cyclic voltammetries of 1 mM solution of complexes **1a-5a** in CH_3CN at 25 ^oC containing 0.1 M $TBAPF_6$ at a scan rate of 0.25 V/s.

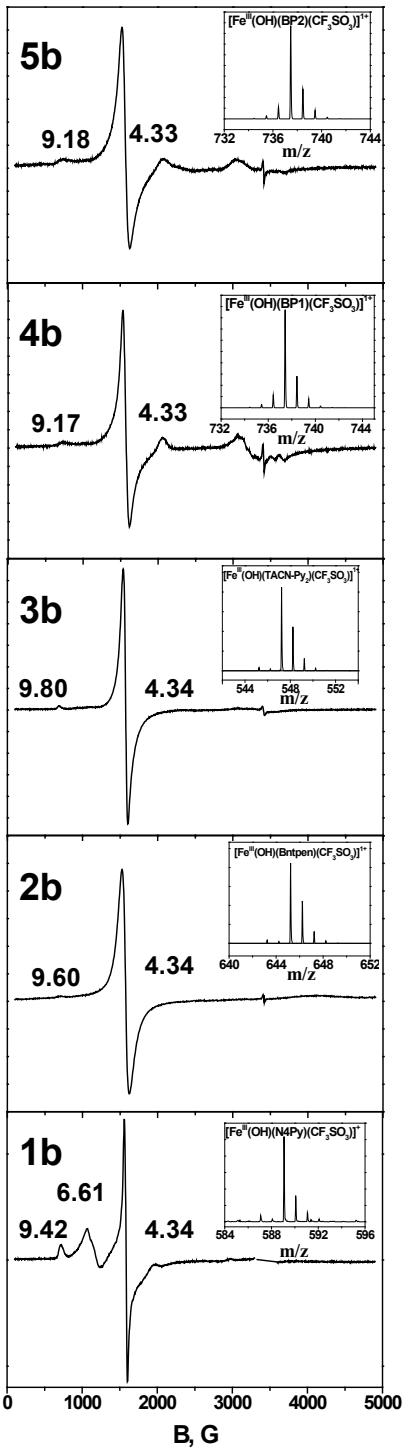

Figure S4. EPR and ESI-MS spectra of **1b** – **5b** obtained by one-electron oxidation of **1a** – **5a** (1.5 mM) in CH_3CN with 0.1 M water. X band EPR spectra were recorded at 9.62 GHz and 10 μW power at 10 K on a Bruker ESR 300 spectrometer equipped with an Oxford ESR 910 liquid helium cryostat and an Oxford temperature controller.

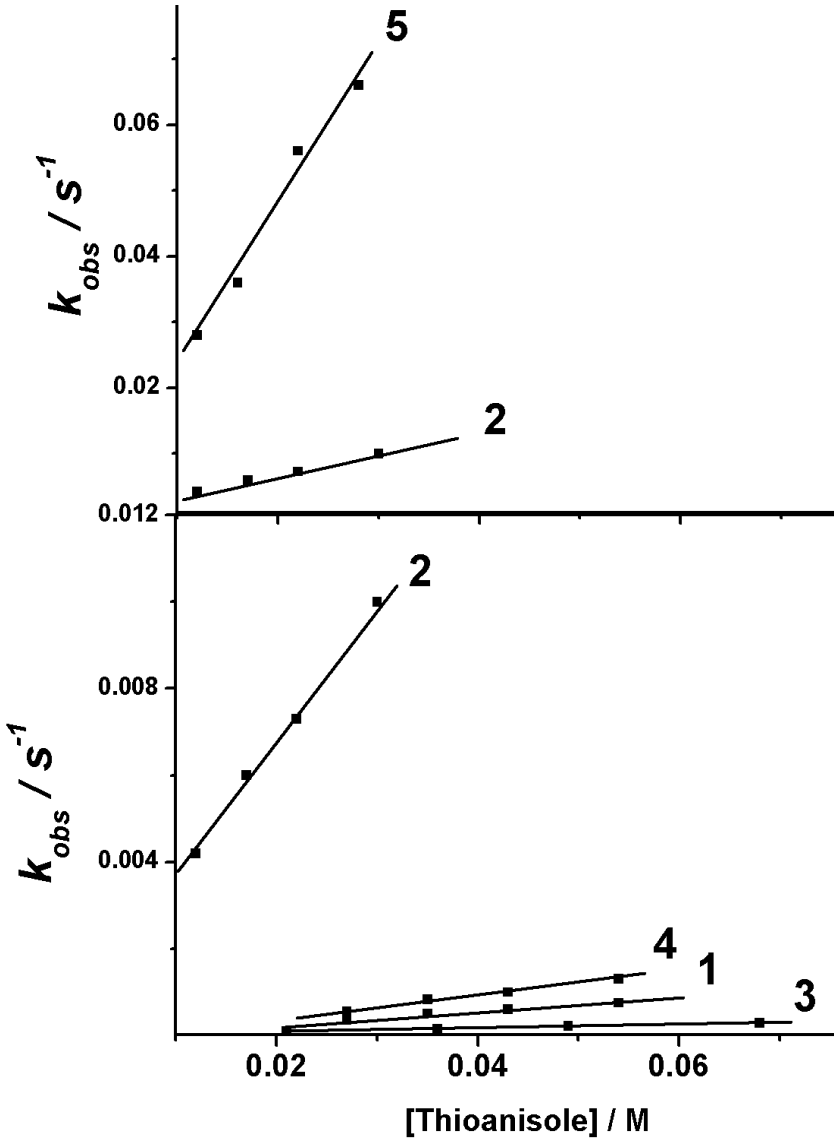

Figure S5. Determination of second order rate constants for the reactions of **1** – **5** with thioanisole in CH_3CN at –10 ^{o}C; relative reactivities of complexes **2** and **5** are shown on top, and for complexes **1 – 4** are shown on bottom.

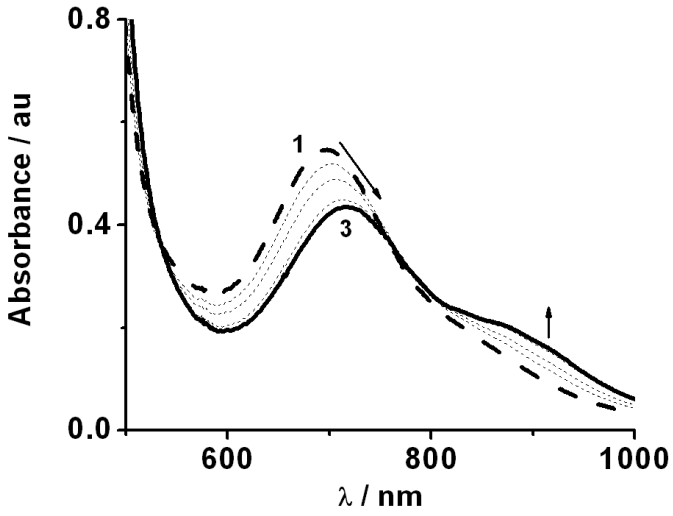

Figure S6. Spectral changes showing the oxo-transfer reaction between **1** and **3a** in CH_3CN at 25 ^{o}C to yield **3** quantitatively

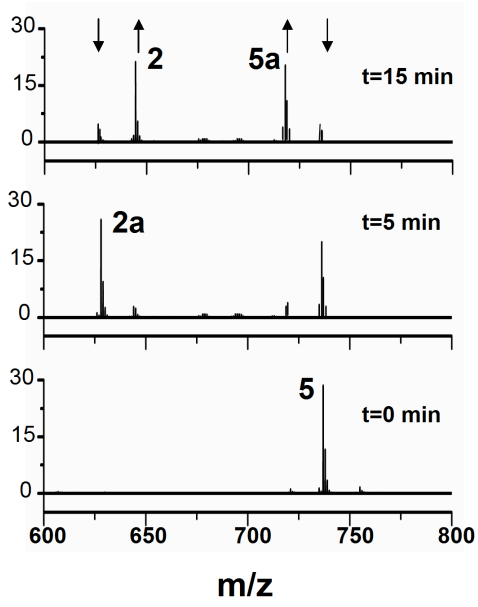

Figure S7. ESI-MS spectral changes associated with the oxo-transfer reaction between **5** and **2a** in CH_3CN at 25 ^{o}C to yield the respective complexes **5a** and **2**.

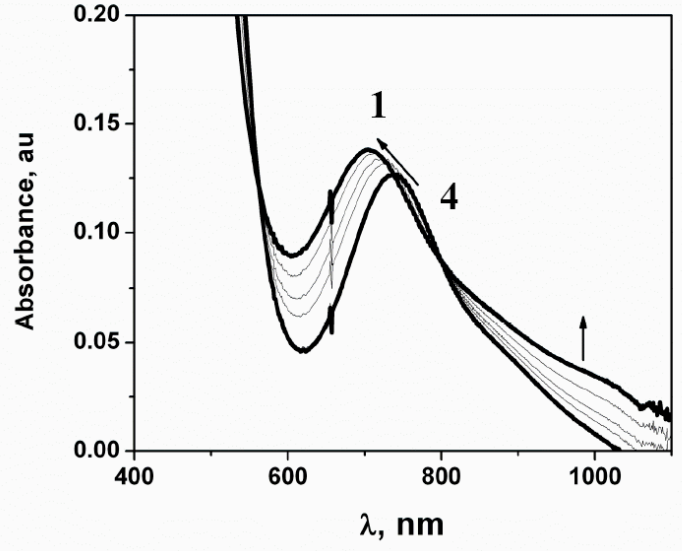

Figure S8. Spectral changes associated with the oxo-transfer reaction between **4** and **1a** in CH_3CN at 25 ^oC yielding **1** quantitatively.

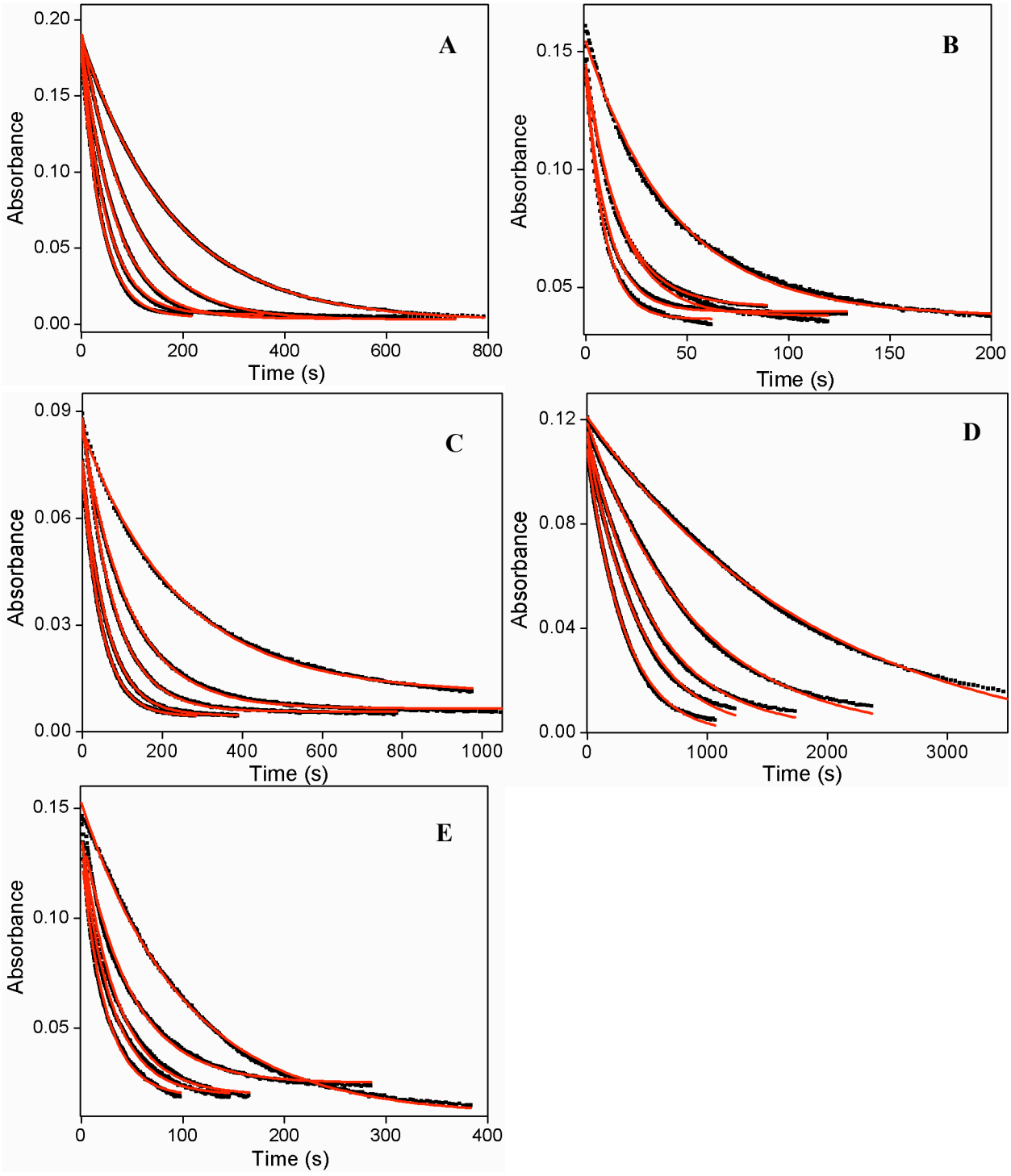

Figure S9a. Kinetic traces (black points) in the course of their reactions with $PhCH_2OH$ for Fe^{IV}=O complexes **1** (A), **2** (B), **3** (C), **4** (D) and **5** (E) in CH_3CN at 25 ^{o}C.

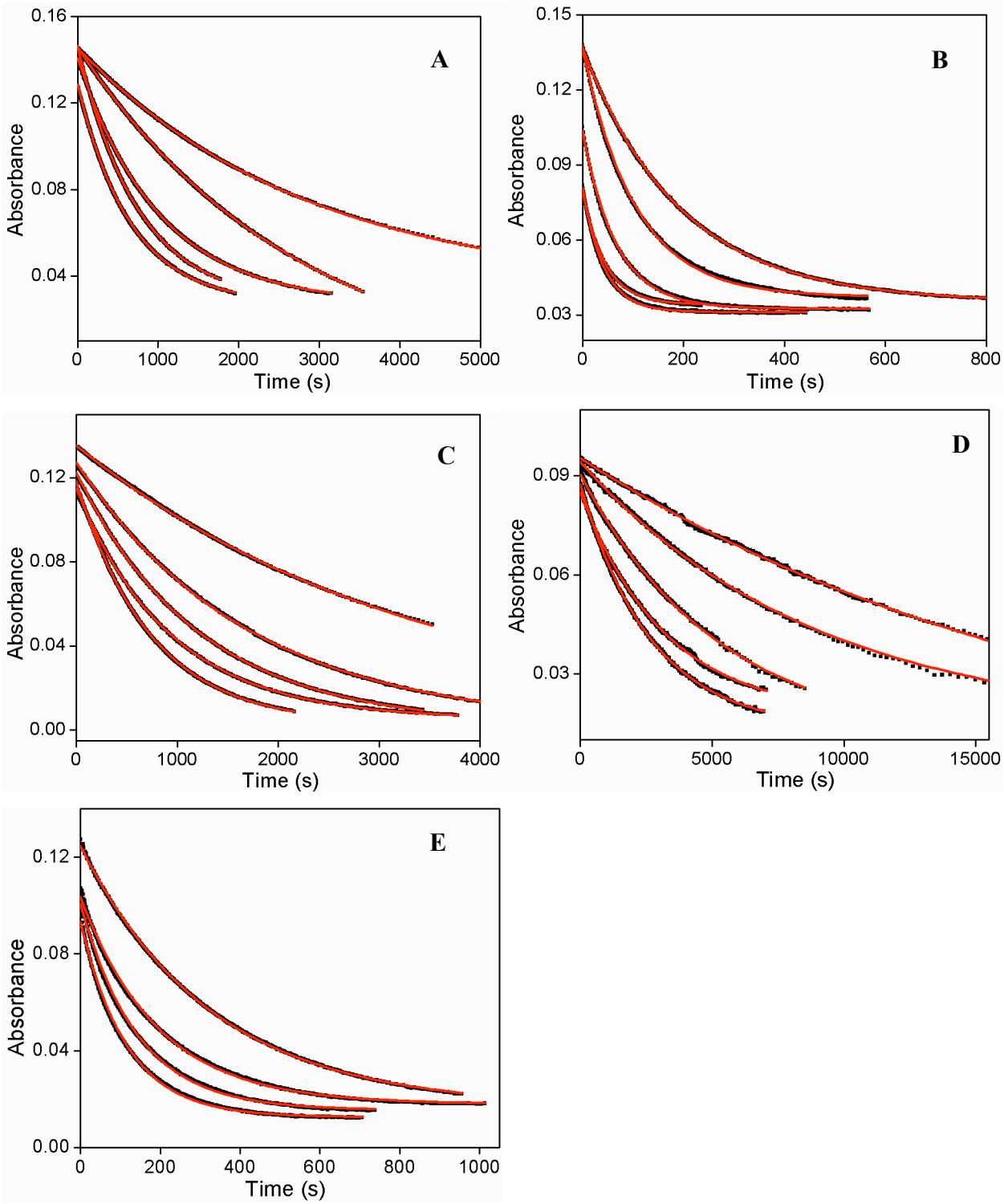

Figure S9b. Kinetic traces (black points) in the course of their reactions with CHD for Fe^{IV}=O complexes **1** (A), **2** (B), **3** (C), **4** (D) and **5** (E) in CH_3CN at -40 ^{o}C.

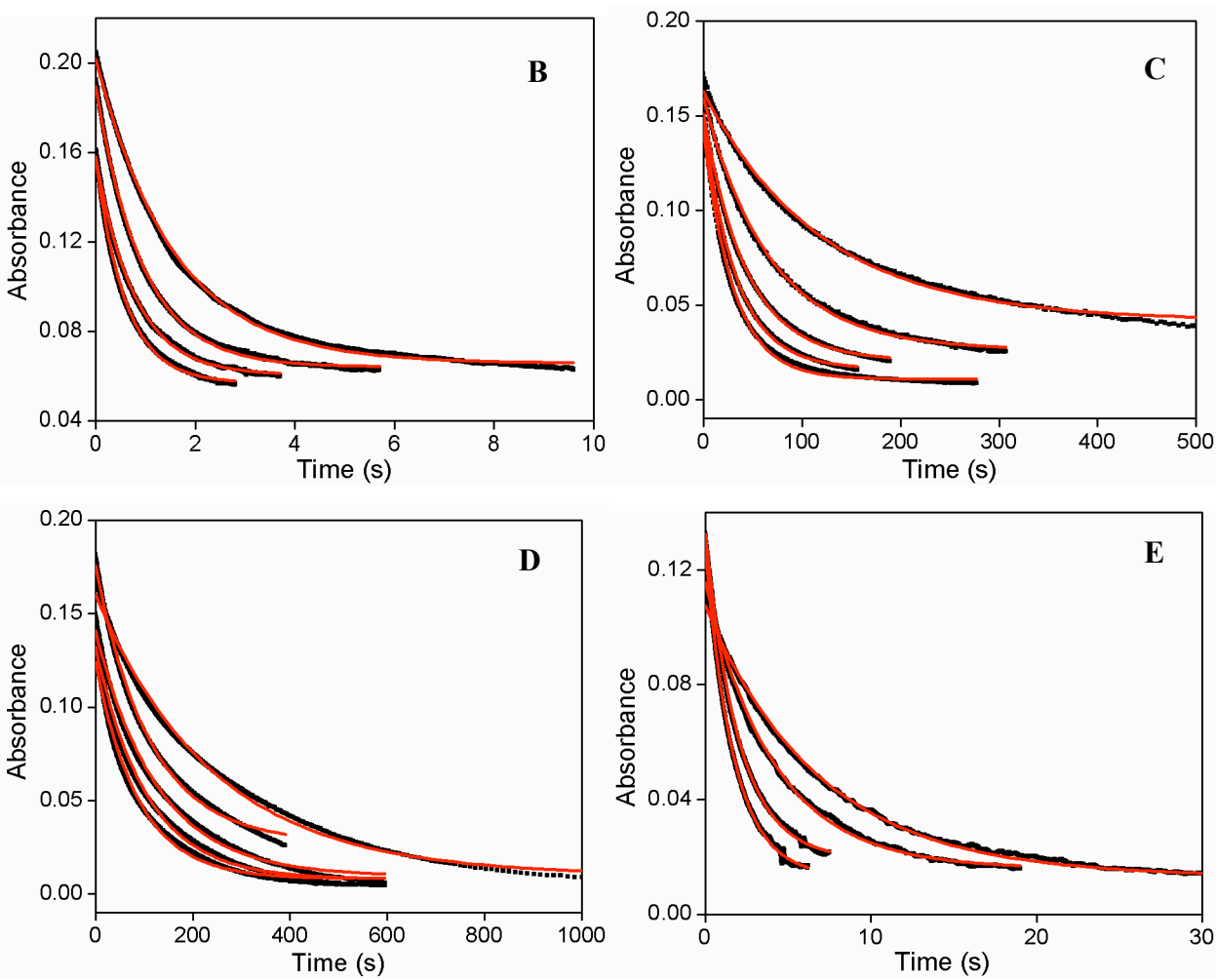

Figure S9c. Kinetic traces (black points) in the course of their reactions with DHA for Fe^{IV}=O complexes **2** (B), **3** (C), **4** (D) and **5** (E) in CH_3CN at 25 ^{o}C.

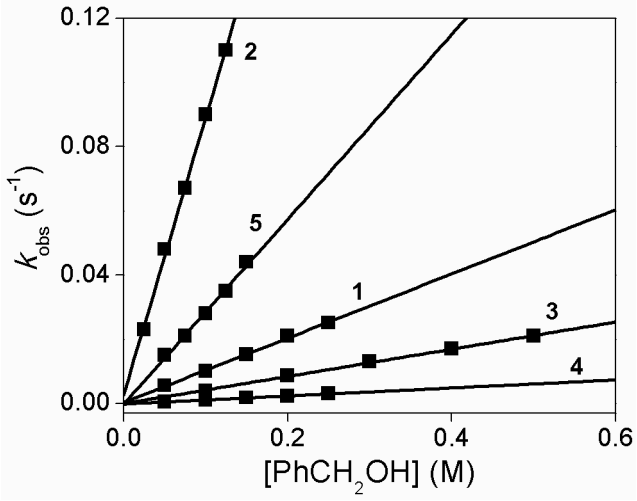

Figure S10. Determination of second order rate constants for the reactions of **1** – **5** with $PhCH_2OH$ in CH_3CN at 25 ^oC.

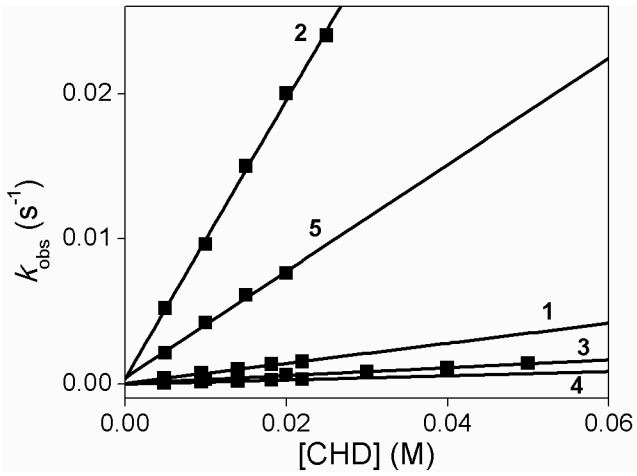

Figure S11. Determination of second order rate constants for the reactions of **1** – **5** with CHD in CH_3CN at -40 ^oC.

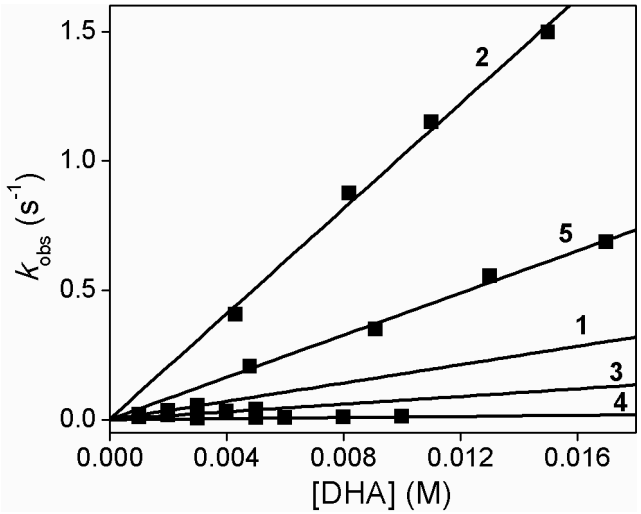

Figure S12. Determination of second order rate constants for the reactions of **1** – **5** with DHA in CH_3CN at 25 ^oC.

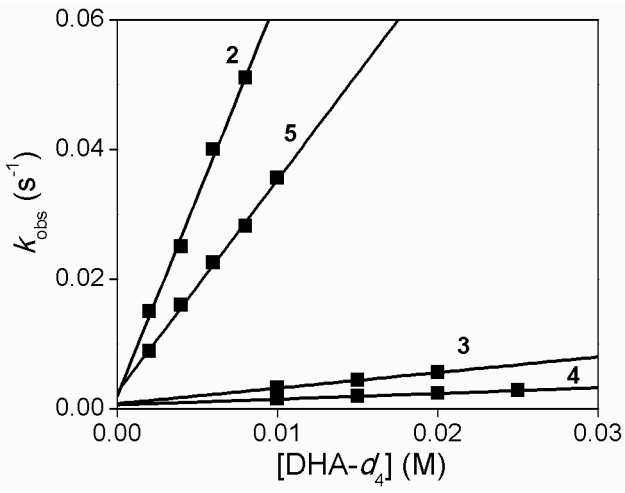

Figure S13. Determination of second order rate constants for the reactions of **2** – **5** with DHA-d_4 in CH_3CN at 25 ^oC.

Table S1. Selected EXAFS Fits for **1**, **3**, **4**, and **5**.[a]

		Fe-O			Fe-N			Fe-N			Fe•••C				
	fit	n	r	σ^2	n	r	σ^2	n	r	σ^2	n	r	σ^2	F [b]	F' [b]
	1				5	1.96	2.7							268	0.47
	2				6	1.95	3.7							344	0.77
	3	1	1.64	2.7	5	1.96	3.0							117	0.10
	4	1	1.64	2.5	4	1.97	1.8							84	0.05
	5	0.9	1.63	2.0	4	1.97	1.8							85	0.05
	6	0.9	1.64	1.9	4	1.97	1.8				4	2.87	10.0	64	0.04
1[c]	7	0.9	1.64	1.9	4	1.97	1.8				5	2.86	12.2	64	0.04
	8	*0.9*	*1.64*	*2.1*	*4*	*1.96*	*1.9*				*4* *4*	*2.76* *2.92*	*2.7* *0.7*	*45*	*0.02*
	9[u]	0.9	1.63	1.9	4	1.97	1.7							302	0.69
	10[u]	0.9	1.63	1.8	4	1.97	1.8				4	2.88	8.2	259	0.59
	11[u]	***0.9***	***1.64***	***2.1***	***4***	***1.97***	***1.8***				***4*** ***4***	***2.75*** ***2.92***	***2.7*** ***0.6***	***212***	***0.49***
	1				5	2.00	2.7							314	0.68
	2				6	2.00	4.1							422	1.22
	3	1	1.64	2.8	4	2.00	1.5							138	0.15
	4	1	1.64	2.5	5	2.00	2.8							164	0.21
	5	*1*	*1.63*	*2.9*	*4*	*2.00*	*1.5*				*5*	*2.89*	*8.2*	*72*	*0.05*
	6	1	1.63	3.0	4	1.99	1.5				6	2.89	9.6	72	0.05
3[d]	7	1	1.63	2.8	4	2.00	1.5				3 3	2.83 2.97	2.8 2.4	71	0.06
	8	1	1.64	2.2	4	2.00	1.7	1	2.29	3.9				118	0.13
	9	1	1.64	2.5	4	2.00	1.6	1	2.31	3.6	5	2.90	8.5	50	0.03
	10[u]	***1***	***1.63***	***3.0***	***4***	***2.00***	***1.4***				***5***	***2.90***	***8.3***	***471***	***2.09***
	11[u]	1	1.63	2.9	4	2.00	1.5				3 3	2.83 2.97	2.0 1.1	462	2.48
	12[u]	1	1.64	2.6	4	2.00	1.5	1	2.30	3.6	5	2.91	8.5	430	2.15
	1				6	2.00	13.6							1466	19.54
	2	1	1.62	4.2	5	1.97	10.9							809	7.27
	3	1	1.62	4.8	4	1.97	8.2							826	7.58
4[e]	4	1	1.64	7.2	3	1.98	3.3	2	2.16	4.1				679	6.59
	6	1	1.64	7.2	3	1.97	3.1	2	2.15	3.9	6	2.94	9.2	101	0.20
	7	*0.7*	*1.64*	*4.0*	*3*	*1.98*	*3.7*	*2*	*2.15*	*4.8*	*6*	*2.94*	*9.8*	*99*	*0.20*
	8[u]	***0.7***	***1.64***	***3.1***	***3***	***1.96***	***3.9***	***2***	***2.13***	***5.1***	***6***	***2.93***	***9.8***	***131***	***0.34***
	1				6	1.92	4.9							1691	27.76
	2	1	1.62	2.4	5	1.94	4.6							689	5.72
	3	1	1.62	2.6	4	1.94	3.4							541	3.53
	4	1	1.63	1.6	4	1.97	3.6	1	2.19	1.3				438	3.05
	5	1	1.63	0.9	1	1.97	-1.8	4	2.04	16.9				476	3.60
5[f]	6	1	1.63	1.6	3	1.97	1.9	2	2.15	8.1				417	2.76
	7	*1*	*1.62*	*1.8*	*4*	*1.97*	*3.3*	*1*	*2.18*	*2.2*	*4*	*2.85*	*7.6*	*146*	*0.50*
	8	1	1.62	2.2	4	1.95	3.4				4	2.81	6.0	220	0.77
	9[u]	***1***	***1.62***	***1.6***	***4***	***1.96***	***3.2***	***1***	***2.16***	***4.6***	***4***	***2.84***	***6.3***	***443***	***4.56***
	10[u]	1	1.62	1.0	4	1.95	5.3				4	2.81	5.2	464	3.42

[a] *r* is in units of Å; σ^2 is in units of 10^{-3} Å^2. All fits are to Fourier-filtered data, except for those with a superscripted u next to the fit number. [b] Goodness-of-fit parameter F defined as $\Sigma(\chi_{exptl} \chi_{calc})^2$, while *F*' is defined as $F^2 / (N_{IDP} - N_{VAR})$, where N_{IDP} is the number of independent data points and N_{VAR} is the number of floated variables in a given fit. *F*' is a test of whether addition of a shell is merited in the fit.[11] [c] Fourier transformation range k = 2 – 14.5 Å^{-1} (resolution = 0.126 Å). Back-transformation range: 0.7 – 3.0 Å. [d] Fourier transformation range k = 2 – 13.5 Å^{-1} (resolution = 0.136 Å). Back-transformation range: 0.7 – 3.1 Å. [e] Fourier transformation range k = 2 – 12 Å^{-1} (resolution = 0.157 Å). Back-transformation range: 1.0 – 3.2 Å. [f] Fourier transformation range k = 2 – 13 Å^{-1} (resolution = 0.142 Å). Back-transformation range: 0.8 – 2.7 Å.

References

1. W. L. F. Armarego and D. D. Perrin, *Purification of Laboratory Chemicals*, Butterworth-Heinemann, Oxford, 1997.
2. H. Saltzman and J. G. Sharefkin, *Organic Syntheses, Vol. V*, Wiley, New York, 1973.
3. M. Lubben, A. Meetsma, E. C. Wilkinson, B. Feringa and L. Que, Jr., *Angew. Chem. Int. Ed.*, 1995, **34**, 1512-1514.
4. J. Kaizer, E. J. Klinker, N. Y. Oh, J.-U. Rohde, W. J. Song, A. Stubna, J. Kim, E. Münck, W. Nam and L. Que, Jr., *J. Am. Chem. Soc.*, 2004, **126**, 472-473.
5. G. Roelfes, V. Vrajmasu, K. Chen, R. Y. N. Ho, J.-U. Rohde, C. Zondervan, R. M. l. Crois, E. P. Schudde, M. Lutz, A. L. Spek, R. Hage, B. L. Feringa, E. Münck and L. Que, Jr., *Inorg. Chem.*, 2003, **42**, 2639-2653.
6. H. Borzel, P. Comba, K. S. Hagen, Y. D. Lampeka, A. Lienke, G. Linti, M. Merz, H. Pritzkow and L. V. Tsymbal, *Inorg. Chim. Acta*, 2002, **337**, 407-419.
7. G. N. George, Stanford Synchrotron Radiation Laboratory, Stanford Linear Accelerator Center, Stanford, 2000.
8. R. C. Scarrow, B. A. Brennan, J. G. Cummings, H. Jin, D. J. Duong, J. T. Kindt and M. J. Nelson, *Biochemistry*, 1996, **35**, 10078-10088.
9. J.-U. Rohde, S. Torelli, X. Shan, M. H. Lim, E. J. Klinker, J. Kaizer, K. Chen, W. Nam and L. Que, Jr., *J. Am. Chem. Soc.*, 2004, **126**, 16750-16761.
10. A. L. A. B. Ravel, J. J. Rehr and S. D. Conradson, *Phys. Rev. B*, 1998, **58**, 7565-7576.
11. P. J. Riggs-Gelasco, T. L. Stemmler and J. E. Penner-Hahn, *Coord. Chem. Rev.*, 1995, **144**, 245-286.
12. M. J. Collins, K. Ray and L. Que, Jr., *Inorg. Chem.*, 2006, **45**, 8009-8011.